Regional Studies in Marine Science 93 (2026) 104718

Contents lists available at ScienceDirect

Regional Studies in Marine Science

journal homepage: www.elsevier.com/locate/rsma

A numerical model approach on floating riverine plastic debris with wind-induced re-drifting process from beaches along the Gulf of Thailand

Pontipa Luadnakrob [a,b,*], María Belén Alfonso [c], Atsuhiko Isobe [c], Tahira Irfan [a], Keiichi Uchida [d], Hisayuki Arakawa [d], Sukchai Arnupapboon [b], Nathacha Changphetphol [b], Suchana Chavanich [e,f], Voranop Viyakarn [f]

[a] Interdisciplinary Graduate School of Engineering Sciences, Kyushu University, 6-1 Kasuga-Koen, Kasuga 816-8580, Japan
[b] Southeast Asian Fisheries Development Center, Phrasamutchedi, Samutprakan 10290, Thailand
[c] Research Institute for Applied Mechanics, Kyushu University, 6-1 Kasuga-Koen, Kasuga 816-8580, Japan
[d] Tokyo University of Marine Science and Technology, 4-5-7 Konan, Minato-ku, Tokyo 108-8477, Japan
[e] Department of Marine Science, Faculty of Science, Chulalongkorn University, Phayathai Road, Pathumwan, Bangkok 10330, Thailand
[f] Aquatic Resources Research Institute, Chulalongkorn University, Phayathai Road, Pathumwan, Bangkok 10330, Thailand

ARTICLE INFO

Keywords:
Re-drifting processes
Beached processes
Offshore-ward wind

ABSTRACT

Southeast Asian countries are widely acknowledged as major sources of plastic waste entering the ocean. The seasonality of floating marine debris abundance in the Gulf of Thailand (GoT) was investigated through visual observations in situ and a particle tracking model (PTM). The observations documented the highest concentration of floating debris (3329 pieces) during the northeasterly monsoon (dry season), characterized by offshore-ward winds on the beaches along the eastern coast. A PTM representing riverine plastic debris was developed to reproduce these observations by incorporating ocean surface currents, horizontal diffusion, Stokes drift, windage, and beaching/re-drifting processes. Two re-drifting processes were examined in the PTM experiments: one where re-drifting occurs on a timescale assigned to each particle with an average of 200 days and another where modeled particles were re-drifting after the onset of offshore-ward winds above the beaches. The latter experiment successfully reproduced the seasonal patterns observed in reality, although re-drifting should occur after 10–60 days from the onset of offshore-ward winds, suggesting that plastic beach litter is prevented from re-drifting immediately due to various obstructions such as beach vegetation. The results indicate that the floating plastic debris observed visually in the GoT does not directly come from rivers but from the beaches where plastic debris accumulates during the onshore-ward winds. This information will support evidence-based measures, such as beach cleanup campaigns, to effectively reduce plastic debris impact in the GoT.

1. Introduction

Plastic pollution has become a pressing global environmental issue, with vast quantities of waste entering marine ecosystems each year. In 2010, an estimated 275 million metric tons (MMT) of plastic waste were generated by 192 coastal countries, with 4.8–12.7 MMT reaching the ocean (Jambeck et al., 2015). Rivers serve as major conduits, transporting between 1.15 and 2.41 MMT of plastic waste annually, with the top 20 polluting rivers—primarily in Asia—accounting for approximately 67 % of this total (Lebreton et al., 2017). Poor waste management, high population densities, and industrial activity drive this pollution, making riverine plastic transport a critical factor in marine debris accumulation.

Southeast Asia is a major contributor to ocean plastic pollution, with five countries, including Thailand, collectively producing approximately 8.9 MMT of mismanaged plastic waste (MPW) annually (Trajano, 2023). Thailand alone generates around 2 MMT of plastic waste each year, but only 27 % is properly managed (ESCAP, 2022). Popular tourist destinations such as Phuket, Krabi, and Ko Samui contribute over 16.8 kilotons of MPW annually, while Nakorn Si Thammarat generates 9,000 tons, with 90 tons flowing directly into waterways (ESCAP, 2022). More recent estimates suggest that 2.83 MMT of municipal solid waste remains uncollected or mismanaged in Thailand's 23 coastal provinces, with approximately 339000 tons being plastic waste and 51,000 tons

* Corresponding author at: Interdisciplinary Graduate School of Engineering Sciences, Kyushu University, 6-1 Kasuga-Koen, Kasuga 816-8580, Japan.
E-mail address: tipa@seafdec.org (P. Luadnakrob).

https://doi.org/10.1016/j.rsma.2025.104718
Received 23 April 2025; Received in revised form 12 December 2025; Accepted 15 December 2025
Available online 18 December 2025

leaking into the ocean each year (UN Environment program and COBSEA, 2023).

The Gulf of Thailand (GoT), a shallow basin averaging 40 m in depth, is particularly vulnerable, with monsoonal winds significantly influencing the movement of floating plastic debris (Guo et al., 2021; Anutaliya, 2023; Nakano et al., 2024). While it is often assumed that the southwest monsoon (April–August) drives debris northeastward and the northeast monsoon (November–February) reverses this flow, transport patterns may be more complex. Riverine input, beach accumulation, re-drifting of stranded debris, and transitional monsoon periods likely play key roles, underscoring the need for further investigation into these dynamics.

Rivers are particularly important in shaping the seasonal distribution of floating plastic debris (Van Emmerik et al., 2019). Thailand's rivers alone may contribute over 51,000 tons of plastic annually to the ocean—far exceeding earlier estimates of 14,000 tons (Lebreton et al., 2017; UN Environment program and COBSEA, 2023). The seasonal variability of river runoff, driven by monsoonal rainfall patterns, further influences the transport and accumulation of plastic debris, underscoring the need to quantify these dynamics more precisely. Beyond riverine input, the exchange of plastic debris between the ocean and beaches is another key factor affecting transport pathways. Particle tracking models (PTMs) have been widely used to simulate these processes (Isobe and Iwasaki, 2022; Irfan et al., 2024), typically relying on predefined timescales based on field studies in mid-latitude regions (Kataoka et al., 2013; Hinata et al., 2017). However, applying these findings to the tropical, monsoon-driven GoT requires adjustments. Persistent onshore and offshore winds likely play a significant role in plastic debris movement, necessitating a wind-dependent exchange process to improve PTM accuracy in this region.

This study aims to enhance our understanding of floating plastic debris behavior in the GoT under different monsoonal conditions. Two PTM experiments were conducted using an e-folding time of 200 days and an assigned delay period to simulate plastic waste dispersal. By integrating numerical modeling with visual observations of marine debris, we refine existing PTMs to better capture beaching and re-

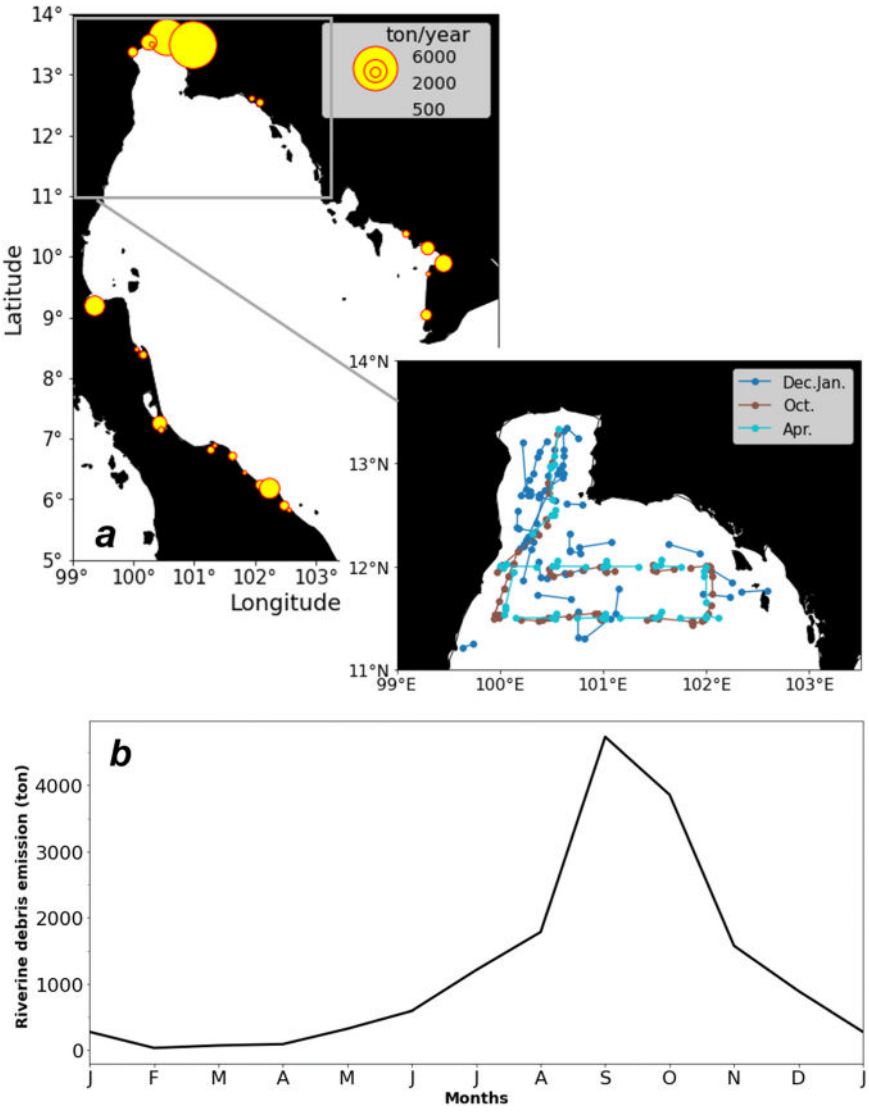

Fig. 1. Study area and riverine plastic debris emissions. The panel (*a*) shows the upper Gulf of Thailand and the northern region, extending from 99°E to 104°E longitude and 11°N to 14°N latitude, where the onboard visual observations were conducted. The insert map illustrates the cruise tracks from multiple surveys in November-December 2019 and January 2022 (dark blue line), October 2023 (brown), and April 2024 (light blue). Dots with the same color as for each month are stations at which we conducted visual surveys of floating objects. Yellow circles at river mouths represent annual riverine plastic debris emissions based on estimates by Lebreton et al. (2017), with circle diameter scaled according to the emission magnitude (as shown in the upper right legend). Panel (*b*) displays the monthly variation in riverine plastic debris emissions throughout a year, also derived from Lebreton et al. (2017).

drifting processes. The findings will provide critical insights into plastic debris pathways and support the development of more effective management strategies to reduce marine plastic pollution in the GoT and surrounding areas.

2. Materials and methods

2.1. Visual observation

The visual observation area covered the northern GoT between 99°E and 104°E in longitude and between 11°N and 14°N in latitude (Fig. 1a). Four observation campaigns were conducted along the prescribed ship tracks during 29th November – 20th December 2019 and 23rd – 28th January 2022 (NE monsoon season), 15th – 22nd October 2023 (transition season), and 3rd – 9th April 2024 (SW monsoon season) using a M. V. *SEAFDEC2* belonging to the Southeast Asian Fisheries Development Center (SEAFDEC).

Two observers from whichever side of the bridge deck had less sea surface reflection attempted to seek flotsam in the daytime along the ship track in the same manner as Randriarilala et al. (2014) and Kuroda et al. (2024). The visual observations were sometimes interrupted by ship operations. Thus, the floating object (flotsam) numbers recorded between the start and end points along each track were converted to flotsam numbers per hour (item/hour). This time-based normalization was dependent on the variation of ship speed over ground during the cruise track (Kuroda et al., 2024). However, because the speed was maintained nearly constant (8.5–10 knots) during the surveys, the number of items per hour is effectively equivalent to the number of items per unit distance and is therefore used here for simplicity (Randriarilala et al., 2014). Before the visual observation along each track, the observers recorded metadata such as speed/direction of the vessel, observation side of the deck (i.e., port or starboard side), sight angle from the horizontal plane, wind speed/direction, sea roughness (ten levels from the calm to stormy), and glare types (glare or cloudy sky reflection). When the observer found a flotsam, the observer recorded the flotsam position coordinates, types (expanded polystyrene foam, food package, glass, metal, plastic bag, plastic bottle, plastic fragments, fishing net, fishery buoy, and unknown objects), sizes visually recognized (< 20 cm, 20 cm - 50 cm, 50 cm - 100 cm, 100 cm - 200 cm, > 200 cm), colors (white, gray, black, blue, green, yellow, orange, red, brown, and clear), and distance from the vessel (calculated from the sight angle, Θ, and the observer's eye height above the sea surface, H) (Fig. 2). The distance was estimated using a trigonometric relation:

$$Distance = H/\tan(\theta)$$

For model purposes, we group the categories of plastic flotsam items according to their different pathways and sources as expanded polystyrene foam, fishing gear (fishing net, fishery buoy, and fishing objects), and other plastic items (food packages, plastic bags, plastic bottles, and plastic fragments).

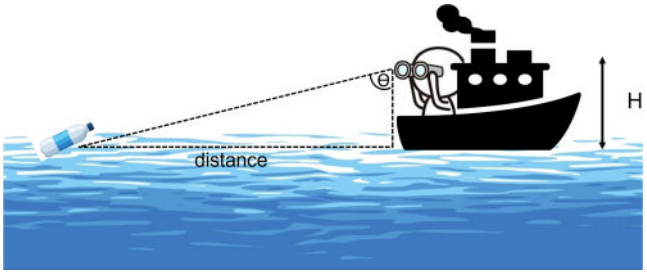

Fig. 2. Schematic representation of the visual observation method used to detect floating plastic debris. An observer, positioned on the vessel at the height (H) above sea level, detects debris at a distance from the vessel. The distance is calculated as shown in the text.

2.2. PTM description

2.2.1. Model descriptions for updating particle positions

In the present study, two-dimensional horizontal PTM experiments were conducted to reproduce the seasonal variation in the abundance (items per hour) and spatial distribution of floating plastic debris observed visually at the sea surface in the GoT. The particle position $[X = (x, y)]$ at time $t + \Delta t$, where Δt the model time step, was calculated according to Isobe et al. (2009) but excluding the fragmentation process of microplastics. Therefore, the present PTM experiments aimed to reproduce the seasonal variation of plastic debris observed in the different monsoon seasons, not its absolute amount, which fragmentation processes would reduce. The positions (X) of each particle at time t were updated as follows:

$$X(t + \Delta t) = X(t) + U\Delta t + R\sqrt{2K\Delta t} \quad (1)$$

where $U[= (u, v)]$ represents the current vectors (including ocean currents, Stoke drift, and windage), R is a random number generated at each time step with an average of 0.0 and a standard deviation of 1.0. The horizontal diffusivity K was defined as $0.01 \times \Delta x^{4/3}$ (Okubo, 1971). Here, the u and v are horizontal current components in the zonal (x) and meridional (y) directions, respectively. The grid spacing Δx was set to $1/12°$ in both latitude and longitude, providing the horizontal currents used in the model. Transport drivers, such as ocean currents (described below), were provided for areas beyond the immediate study domain (see map in Fig. 1a), allowing particle tracking computations to continue even after particles exited the target area.

In the present PTM, particles were transported by surface ocean currents, Stokes drift induced by wind waves, and windage. All forcing data were monthly averages from daily records spanning 1993–2018. Ocean surface currents were obtained from the Hybrid Coordinate Ocean Model (HYCOM; https://www.hycom.org). Stokes drift was calculated using the University of Miami wave model v1.0.1 (Donelan et al., 2012), driven by monthly-averaged wind data from the Japanese Ocean Flux Data Sets with Use of Remote Sensing Observations (J-OFURO), with a horizontal resolution of 0.25° at 10 m above the sea surface (Tomita et al., 2019). The ETOPO1 dataset (Amante and Eakins, 2009) provided the bottom topography and coastlines for the wave model. Windage, representing the excursion owing to drag force exerted by winds directly on floating particles was computed using the monthly satellite-derived wind vectors from J-OFURO. To incorporate the windage into the PTM algorithm, we applied Richardson's relationship (Richardson, 1997) between wind speed at 10 m (W_{10}) and windage speed (U_w) as follows:

$$U_w = \sqrt{\rho_a/\rho_w \bullet C_a/C_w \bullet A_a/A_w} \bullet W_{10} \quad (2)$$

where ρ_a and ρ_w are the densities of air and seawater, respectively; C_a and C_w are the drag coefficients in the air and seawater; and A_a and A_w are the horizontally projected areas of debris above and below the sea surface, respectively. The ratios were set as $\rho_a/\rho_w = 1.15 \times 10^{-3}$ and $C_a/C_w = 1.0$. The ratio $A_a/A_w$was randomly assigned values between 0 and 10 (with 50 % of the values falling between 0 and 1) to represent the diverse characteristics of different types of debris (Kako et al., 2010). This random assignment reflects the varying shapes, sizes, and buoyancies of different types of floating plastic debris (e.g., plastic bags, bottles, and foam), which influence the degree of exposure above the water surface and hence the wind drag acting on the particles. As a result, the PTM accounts for particle-specific windage effects, thereby incorporating part of the physical variability of floating plastics without explicitly modeling detailed material composition or degradation processes. The monthly average ocean currents and Stokes drift were provided at each $1/12° \times 1/12°$ grid cell at mid-month, while wind vectors were simultaneously given to each $1° \times 1°$ grid cell. Surface ocean currents, Stokes drift, and windage were linearly interpolated in both

time and space at each particle position for every time step and then combined to obtain the total surface current vector (U) used in Eq. (1). Monthly datasets for currents and winds were cyclically reused, irrespective of the simulation year.

2.2.2. Plastic debris emission imposed on the PTM

In the present experiments, monthly data of the riverine plastic debris emission from Lebreton et al. (2017) were applied to the river mouths across the GoT (Fig. 1a). In this study, we selected the river mouths with emissions greater than 40 tons per year, which account for 96 % of the total plastic emission into the GoT. Emissions were imposed once each month, on the first day of the month. One ton of plastic debris was modeled as a single particle in the PTM. The plastic emission from rivers across the GoT exhibited the maximum (or minimum) in September (or February), corresponding with the seasonality of river runoff (Fig. 1b). This monthly variation of plastic debris emission was repeatedly applied to the rivers, regardless of the year. The PTM experiments began with a domain devoid of particles representing plastic debris and continued until the end of year 6, when the seasonality of particle amounts in the GoT became nearly stable (as shown later in subsection 3.2).

2.2.3. Model description for particle exchange between ocean and beach domains

Two different scenarios were examined in the PTM experiments to simulate re-drifting processes from beaches to the ocean domain (Table 1).

In the first PTM experiment, particles that were washed ashore on beaches re-drifted on a timescale assigned to each particle at its generation. In the second case, the occurrence of re-drifting depends on wind directions above the beach where the particles stayed. In both cases, particles in the ocean domain were regarded as washed ashore on beaches once they were positioned on beaches via the transportation by Eq. (1).

In the first scenario, particles re-drifting occur on a timescale (τ^*) assigned to each particle at the time of its generation in line with exponential random numbers. This timescale followed an exponential distribution $e^{\frac{-\tau^*}{\tau}}$, with an e-folding time of $\tau = 200$ days based on observations by Kataoka et al. (2013), who monitored temporal changes in a specific type of buoy stranded on a Japanese beach. The present experiment was conducted like Irfan et al. (2024), where the time since beaching was tracked individually for each particle. When the elapsed time exceeded τ^*, the particle re-drifted to the location where the particle existed just before beaching. The e-folding timescale of 200 days was obtained experimentally on a single beach, so to assess the model sensitivity experiments were conducted by changing the timescale from 100 to 300 days to examine the dependence of the timescale on modeled results.

In the second scenario, re-drifting depended on persistent offshore-ward wind conditions during a 'delayed period' prescribed in the experiment. It is reasonable to incorporate the wind-induced re-drifting into the PTM experiments in tropics and subtropics under the monsoon condition varying in seasons because offshore-ward winds persistently continuing for a few months over the beach provide a favorable condition for beach plastic debris to move in the offshore-ward direction and vice versa. However, it is not easy to uniquely determine how long the offshore-ward winds need to blow persistently for re-drifting of beach plastic debris. Re-drifting to the ocean just at the onset of offshore-ward winds seems to be unlikely because entanglement in beach vegetation ("Christmas tree effect"; Williams and Simmons, 1996; Ivar do Sul et al., 2014) and/or burial in the sand (Williams and Tudor, 2001; Asensio-Montesinos et al., 2019) can delay or inhibit re-drifting. A particle on a beach returns to the ocean domain if offshore-ward winds over the beach continue for a longer time than a delayed period prescribed in the present PTM.

In this experiment, the delay period was tested at 0, 10, 30, 60, and 90 days. A longer delay reduced the likelihood of particles re-entering the ocean, due to increased trapping in the coastal environment. If the wind direction reversed before reaching the required delay, the countdown for that particle was reset. Although 0 days is not realistic, it was included for comparison, while 90 days was selected as the upper bound, since longer delays would likely prevent re-drifting due to seasonal wind reversals. The appropriate delay period was determined based on the model's ability to realistically reproduce the seasonal variation in floating plastic debris, as observed visually.

Table 1
Summary of PTM experiment design and conditions.

Experiments	Re-drifting scenarios	Delay period	Ref.
1st PTM experiment	Wind-independent	200 days*	Kataoka et al. (2013)
2nd PTM experiment	Wind-dependent	0, 10, 30, 60, and 90 days.	Present study

* The delay period was given to the model as the e-folding time of the re-drifting timescale assigned randomly to each particle (see the text)

3. Results

3.1. Visual observations

The visual observations revealed the highest number (3329 items) of total plastic debris during the NE monsoon (December and January), while the lowest (937 items) was observed during the southerly monsoon (April, hereinafter included in the SW monsoon season for simplicity) (Fig. 3). Among the types of debris, other plastics were the most frequently found in all periods, followed by expanded polystyrene foam (Table 2). The highest percentage of other plastics was recorded during the transition season (October; 80.9 %), followed by 67.3 % during the NE monsoon and 59.6 % during the SW monsoon. The highest percentages of foam (34.0 %) and fishing gear (6.4 %) were observed during the SW monsoon, followed by the NE monsoon (28.5 % and 4.2 %, respectively), and lastly, during the transition season (18.0 % and 1.1 %). The composition of observed floating debris by type, size, and color during each survey period is summarized in Table 3. Foam and other plastics dominated across all seasons, while most items were smaller than 20 cm and predominantly white and transparent in color. A more detailed breakdown of debris categories, including fishing gear and plastic subcategories as well as glass and metal items, is provided in Supplementary Tables S1–S2.

Floating plastic debris was found widely and homogeneously across the survey area during both the SW and NE monsoons (Fig. 3a, c). As mentioned above, the number of floating debris during the SW monsoon was significantly lower compared to the NE monsoon. Higher concentrations (item/hour) were revealed on the western side of the GoT in the transition season (October; Fig. 3b). These high concentrations seem to appear in the southward ocean currents along the western boundary in these seasons (arrows in the background of Fig. 3). In October, both large river discharge (Fig. 1b) and large percentage of other plastics (Table 2) suggested that riverine plastic debris generated on the bay head moved southward along the western boundary of the GoT. However, the predominance on the western side becomes unclear despite the intensification of the southward ocean boundary current in the NE monsoon season (December and January; Fig. 3c), suggesting that floating plastic debris found during the surveys did not originate from the rivers during the same period.

3.2. The PTM experiments

A clear seasonal variation in the modeled particle counts, integrated across the areas north of 11°N (consistent with observations), emerged

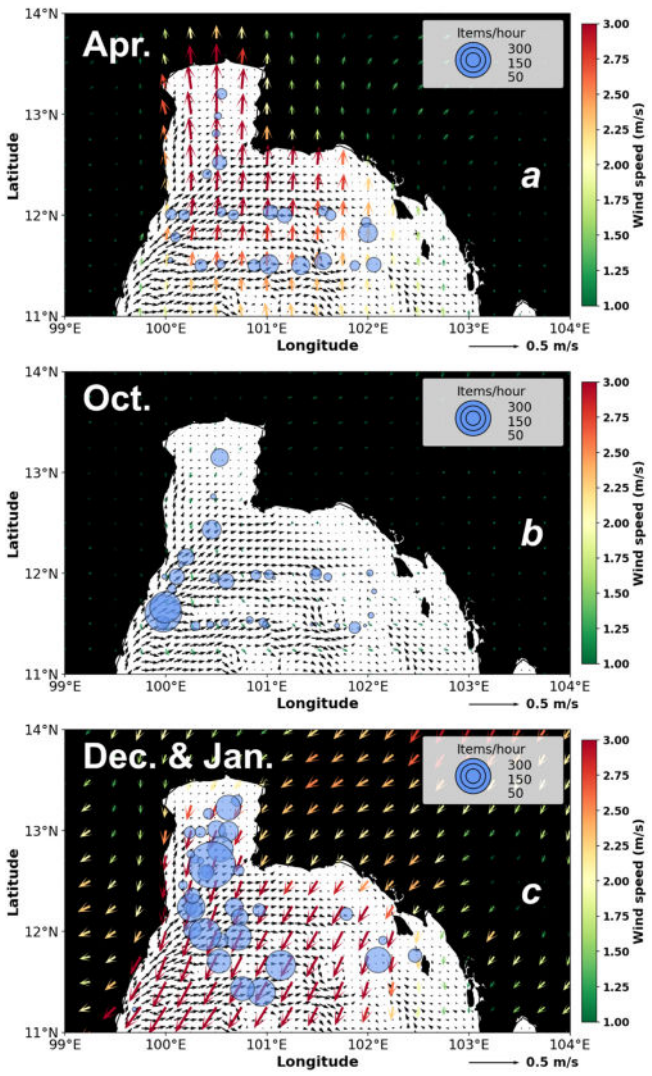

Fig. 3. Abundance of visually observed plastic debris during (*a*) the SW monsoon (April), (*b*) transition season (October), and (*c*) NE monsoon (December and January). The size of the blue circles represents the number of plastic items observed per unit hour, scaled according to the legend at the right. Colored arrows indicate wind vectors (m/s, see right scale), while black arrows represent ocean currents, with corresponding velocity scales shown in the lower right corner of each panel.

Table 2
Total counts of floating debris items recorded through visual observation during the Southwest (SW) monsoon, transition season, and Northeast (NE) monsoon.

Items	SW monsoon (Apr)	Transition season (Oct)	NE monsoon (Dec-Jan)
Foam	319 (34.0 %)	236 (18.0 %)	949 (28.5 %)
Fishing gear	60 (6.4 %)	15 (1.1 %)	141 (4.2 %)
Other plastic	558 (59.6 %)	1061 (80.9 %)	2239 (67.3 %)
Total	**937**	**1312**	**3329**

over the GoT from year 5 onward in both PTM experiments. Therefore, we focused on the results from the last two years of the six-year computation (Fig. 4). For comparison, the numbers of plastic debris visually counted during the three surveys are shown repeatedly over the same two-year periods. To emphasize seasonal variation, the modeled time series was detrended using a least-squares linear regression.

Table 3
Percentages of plastic debris categories during three survey periods.

Categories	Subcategories	Seasons		
		SW Monsoon (Apr)	Transition (Oct)	NE Monsoon (Dec–Jan)
Types	Foam	34.1	18.0	28.5
	Fishing gear[*1]	6.4	1.1	4.2
	Other plastics[*2]	59.6	80.9	67.2
Sizes	< 20 cm	66.3	44.0	67.4
	20–50 cm	29.6	50.4	30.8
	50–100 cm	2.9	4.5	1.5
	100–200 cm	1.0	0.6	0.2
	> 200 cm	0.2	0.5	0.1
Colors	White	60.0	66.3	56.5
	Transparent	22.3	20.3	28.6
	Red	2.9	2.7	4.1
	Yellow	5.6	2.7	3.7
	Other[*3]	9.1	8.0	7.2

[*1] nets, buoys, ropes [*2]bags, bottles, fragments, food packaging
[*3] Black, Blue, Gray, Green, Brown, Orange

A linear trend was present in the modeled particle counts due to the exclusion of removal processes such as fragmentation into microplastics, burial in sand, and entanglement in beach vegetation. In the first experiment, it was difficult to reproduce a rapid increase of plastic counts observed visually during the NE monsoon season (December and January) due to a 1–2 month time lag, regardless of whether the re-drifting timescale was set between 100 and 300 days (Fig. 4a). In contrast, in the second experiment time lag was reduced to one month or less with 0-day delayed period. However, there was an unexpected peak from March to May, during which field surveys recorded low plastic counts. These discrepancies suggest that further refinement of the PTM is necessary to better replicate the observed patterns of plastic debris.

Incorporating a delay period in the re-drifting process of beached plastic debris is a reasonable approach, as beach features such as undulations, vegetation, and natural debris can hinder immediate return to the ocean. To better capture this behavior, we introduced delay periods ranging from 0 to 90 days in the second PTM experiments (Fig. 5). A distinct winter peak in December emerged in simulations with short delays (less than 10 days; Fig. 5a, b). In the 10-day delay experiment, the March–May peak observed under the 0-day delay condition shifted to June during the SW monsoon. However, the accuracy of this shift could remain uncertain due to a lack of observational data for that period (Fig. 5b).

With longer delays of 30 and 60 days, the SW monsoon peaks were reduced in magnitude, while a more pronounced peak appeared during the NE monsoon (December–January), aligning more closely with field observations (Fig. 5c, d). In contrast, the 90-day delay experiment produced a peak in February, one to two months later than observed, indicating a reduced agreement with real-world data (Fig. 5e). These results suggest that moderate delay periods (e.g., 30–60 days) may best capture the dynamics of re-drifting plastic debris under monsoonal conditions.

4. Discussion

4.1. Potential sources of floating plastic debris observed in the GoT

The detrended particle counts from the last two years of the second experiment demonstrated that the winter increase of floating particles was in phase with the decrease in beached particles (Fig. 6 for a 30-day delayed period). Notably, the amplitude of the seasonal variation in beaching during the NE monsoon (November to February) contributed to the increase in floating particles during the same period. The modeled result was consistent with the visual observations, which recorded the

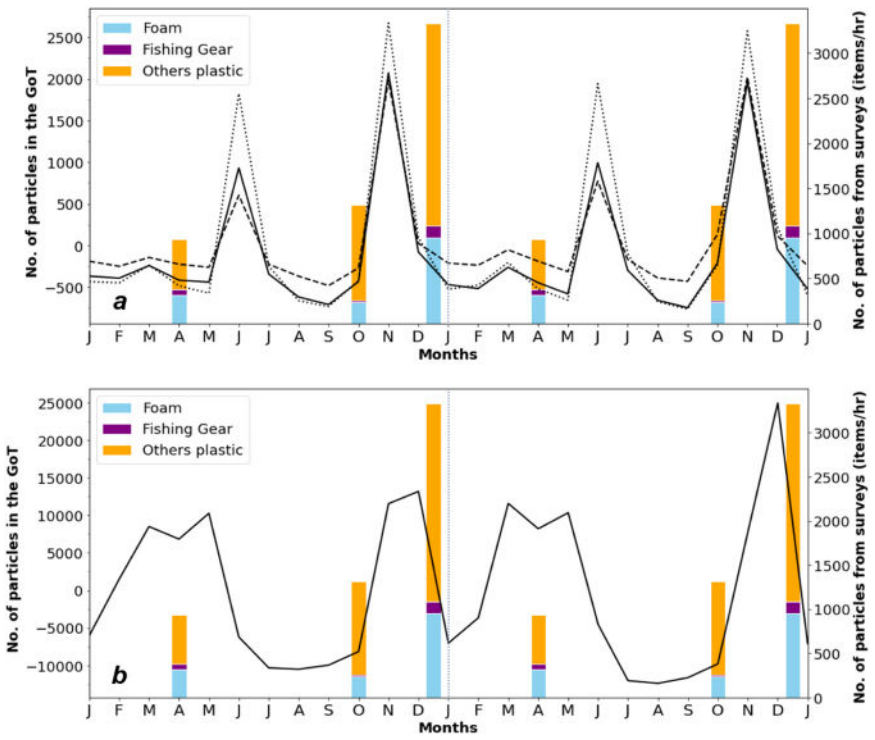

Fig. 4. Comparison between observed and modeled abundance of floating debris in the northern GoT (insert map in Fig. 1). Hourly numbers of floating debris visually observed along the survey track (bars; right ordinate) are compared with detrended time series of modeled particle mass from the PTM (lines; left ordinate). In the bar chart, different colors represent categories of observed debris as shown in the legend. The results of the first PTM experiment are shown in panel (*a*) with different residence times of 100 (dotted), 200 (solid), and 300 (broken lines) days. Panel (*b*) shows the results for the second experiment with the delayed period of 0 day. Both panels display modeled data for the last two years of simulation, while the same observed data are repeated for comparison.

highest number of flotsam during the NE monsoon (December and January; Fig. 3), although corresponding beach surveys were not conducted in the present study.

According to the results, the number of beached particles begins to accumulate from the mid-SW monsoon (June) until the onset of the NE monsoon (November), and these beached particles are likely the source of the floating particles observed during NE monsoon season (hence, floating plastic debris found in the winter survey). A similar seasonal pattern was reported by Irfan et al. (2024), who used a PTM to evaluate riverine plastic debris in the Indian Ocean. They found that the beached particles increased from July to October and decreased from November to January, which aligns with our findings. While their modeling approach closely resembles ours, a key difference is that our results were validated exclusively through visual observations of floating debris, due to the lack of beach survey data in the GoT, which may enhance our results. Monchanin et al. (2024) investigated marine macrodebris on Koh Mun Nai in the eastern GoT and found higher debris densities from February to April compared to October to December. This contrast with our findings, which showed lower beached particles between January and June. This discrepancy may be due to Koh Mun Nai's unique characteristics as a small, uninhabited island, which may influence debris accumulation differently than mainland beaches.

The month-to-month differences in the beached particles counts provide insights into the processes driving particle accumulation on beaches (Fig. 7). The difference between August and July (August minus July, and similarly for the other comparisons), indicates a higher concentration of beached particles along the eastern side of the GoT (Fig. 7a) likely resulting from floating particles being pushed ashore by the prevailing SW monsoon winds. The difference between October and September highlights a large accumulation that occurred on the beaches in the northernmost gulf during the transition season (Fig. 7b). In addition, the accumulation was extended southward along the western coasts of the GoT. These accumulation patterns were consistent with the peak riverine emission during the transition season (Fig. 1b), and visual observations of land-based debris on the western GoT in October (Fig. 3 and Table 2). This suggests that the beached particles accumulating in the upper gulf during the transition season likely originated from increased riverine inputs. In contrast, the difference between December and November (Fig. 7c) shows a near mirror image of the August and July pattern (Fig. 7a), reflecting the reversal of monsoonal wind direction during the NE monsoon. The decrease in beached particles along the eastern coasts of the GoT suggests that these locations may serve as sources of re-floating plastic debris during the winter months.

A series of October, November, and December maps of floating particles in the second experiment, with a 30-day time lag, demonstrate the sources of plastic debris visualized in winter (Fig. 8). These maps also shown the significant accumulation of beached particles along the northern and eastern coastlines of the GoT. Interestingly, the floating particles increased (Fig. 3) as the NE monsoon wind intensified from October to November, suggesting that the wintertime floating debris in the GoT is not solely the result of riverine inputs occurring during that season. Instead, previously beached plastic debris may also be remobilized by offshore-ward winds and transported back into the water. In addition, seasonal sea-level variations may further enhance debris re-drifting during the NE monsoon. The mean sea level in the GoT is typically higher during the NE monsoon than during the SW monsoon (Saramul and Ezer, 2014; Narenpitak et al., 2025), as a result of wind setup and regional circulation patterns. Elevated sea levels can facilitate the re-drifting of stranded debris, allowing previously beached material to be more easily washed back into the sea. This mechanism likely contributes to the observed winter peak of floating debris in the GoT.

This interpretation is consistent with the findings of Harris et al. (2021), who used GIS-based analyses to demonstrate that 52 % of plastic waste transported by rivers to the ocean tends to accumulate along river-dominated coastlines. Similarly, Zhang et al. (2022) found that most plastic debris originating from terrestrial sources remains stranded

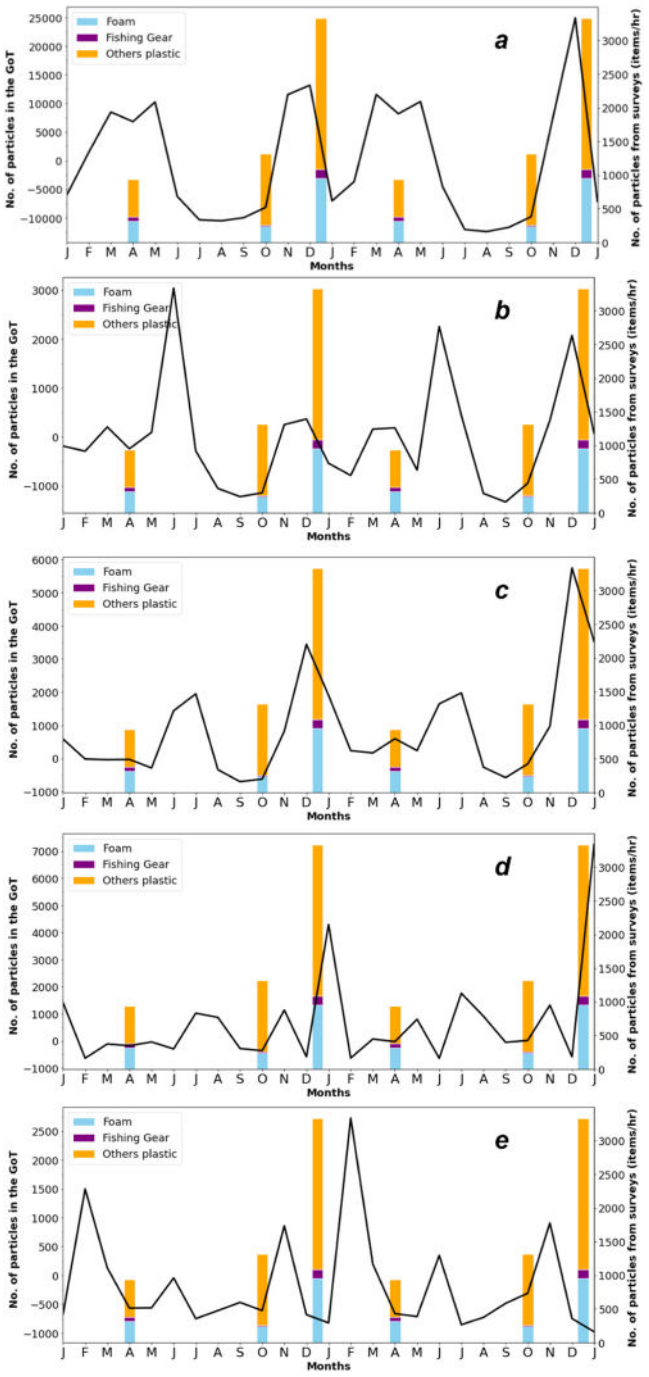

Fig. 5. Comparison between modeled and observed abundance of floating debris in the GoT from the second PTM experiment. Modeled results (lines; left ordinate) are shown for delayed periods of 0 days (*a*), 10 days (*b*), 30 days (*c*), 60 days (*d*), and 90 days (*e*), together with observed data (bars; right ordinate).

on the beach, emphasizing that the interactions between land and sea make tracing the sources of plastic pollution particularly complex. Further supporting evidence comes from Yin et al. (2020), who investigated the dynamics of anthropogenic marine debris accumulation in urban and peri-urban mangroves on Penang Island, Malaysia. Their transects survey study showed that mangrove canopy and root structures effectively retained debris within the interior, whereas debris closer to the shoreline is more likely to be sorted and returned to the sea, particularly smaller plastic fragments. They also observed that plastics were the dominant debris type across all sampling sites, consistent with global trends reported in beach and mangrove environments.

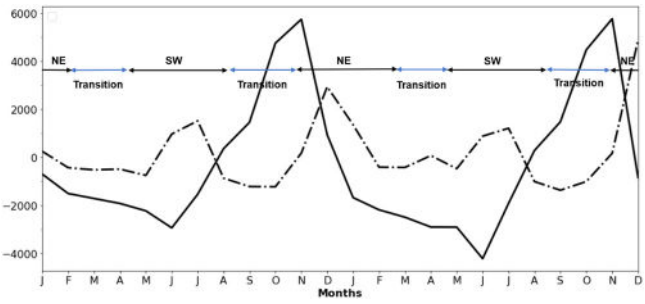

Fig. 6. Detrended monthly variations for modeled particles in the ocean (single-pointed line) and on the beaches (solid line) in the last two years in the second experiment with the delayed period of 30 days. The variations were computed for the same area in Fig. 4. The periods corresponding to the Northeast (NE) monsoon, transition season, and Southwest (SW) monsoon in the Gulf of Thailand (GoT) are also indicated.

In particular, the eastern beaches become significant sources of floating plastic debris during the NE monsoon. The modeled results are consistent with the observations, such that the floating plastic debris concentration along the western coasts in October spread over the entire Gulf in the subsequent months (Fig. 3). This suggests that well-planned beach cleanup campaigns along the northern and eastern coasts could play a critical role in reducing ocean plastics in the GoT by removing beached plastic debris before it is re-drifted into the ocean.

The peaks also appeared in the SW monsoon seasons because the particles washed ashore along the western coast and re-drifted into the ocean (see the negative difference along the western coast in Fig. 7a). However, the height of peaks in the SW monsoon season was sensitive to the choice of delayed periods (Fig. 5b, c, and d). This summer peak was not robust in the present PTM because the drifting particles were carried from the GoT to the outer ocean due to the southward boundary current along the western coast in the NE monsoon (Fig. 3c), and because particles moving onto the western coast during the NE monsoon become therefore smaller than those washed ashore on the eastern coast during SW monsoon season. Although the peak of floating debris is likely to appear in June and July in the actual ocean in the same fashion of the PTMs (Fig. 5b, c, and d), its magnitude compared to the winter peak was unable to be conclusive in the present study due to both lack of field surveys and uncertainty of the delayed period. In addition, during the NE monsoon, riverine debris is transported southward along the western coast due to prevailing northeasterly winds and associated surface currents, whose speed and direction vary both in space and time due to wind fluctuations, local current variability, and coastal morphology in the reality. Consequently, the re-entry and redistribution of beached debris across the GoT can vary substantially in both time and space, resulting in unstable peaks during the subsequent SW monsoon season.

4.2. Suggestion for additional field surveys to determine the delayed period

Two different approaches were applied to model the re-drifting of plastic debris from beaches back to the ocean. Among them, the first experiment, with an average residual time, appears inappropriate for the GoT, a semi-enclosed gulf under a monsoon system in the subtropics, irrespective of the residence time selected (Fig. 4a). The residual time of 200 days was experimentally estimated for a Japanese beach (Kataoka et al., 2013), where litter may return to the ocean year-round due to natural events such as storm surges caused by subweekly-scale extratropical cyclones during spring tides. The removal of beach litter under these conditions was demonstrated using webcam monitoring by Kako et al. (2018), who documented mid-latitude storm-driven mobilization (see their Fig. 8 for photographs taken on a beach along the western coast of the United States). In such settings, the strong

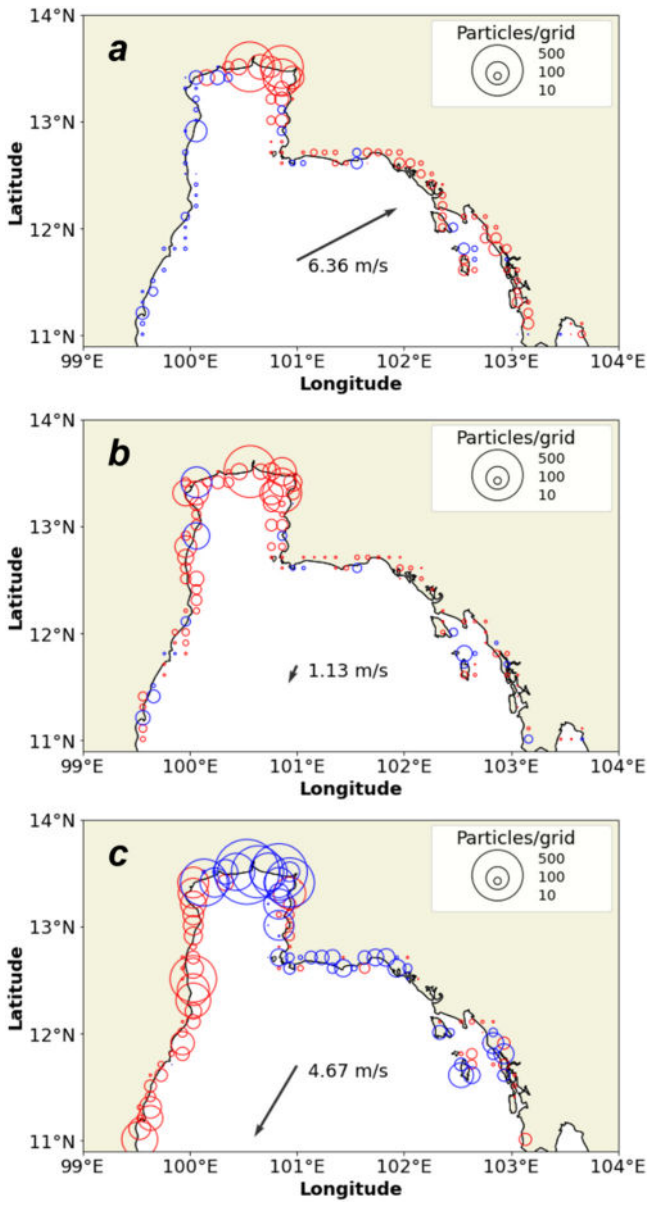

Fig. 7. Monthly differences in beached particle average abundance in the second PTM experiment with a 30-day delayed period between successive months: (*a*) August minus July, (*b*) October minus September, and (*c*) December minus November. Red circles indicate positive differences (increased beached particles), while blue circles represent negative differences (decreased beached particles). The diameter of each circle corresponds to the number of particles per 1/10° × 1/10° grid cell, with reference scales shown in the upper right corner of each panel. Wind vectors averaged over the later month of each pair are overlaid, with wind speed values also indicated.

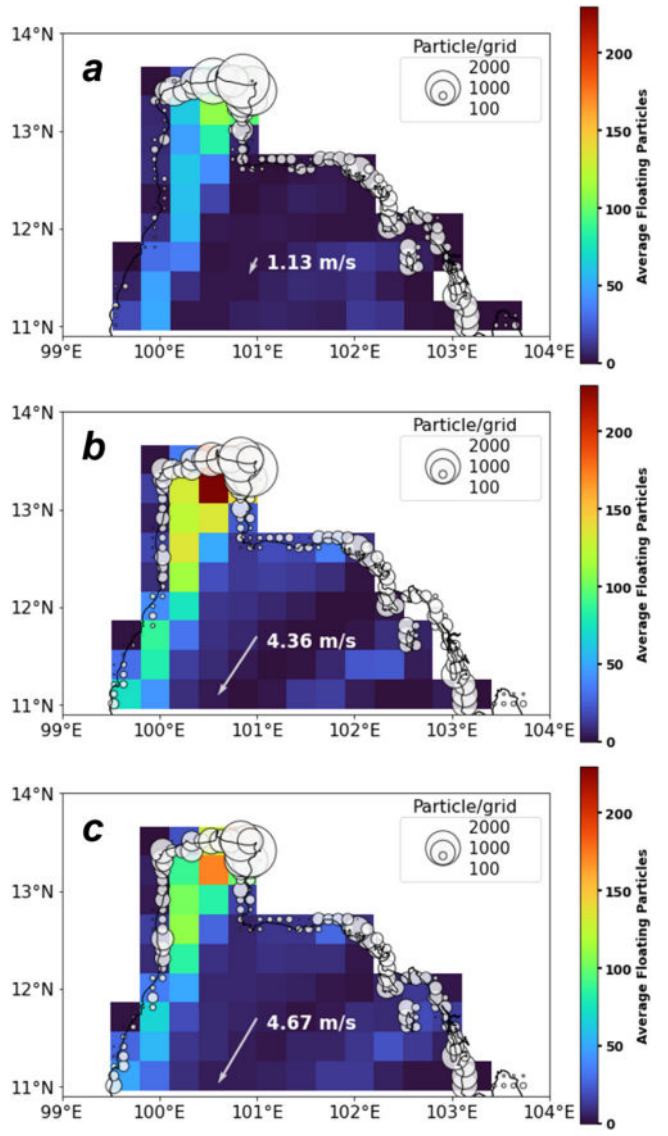

Fig. 8. Monthly average numbers of floating and beached particles in the second PTM experiment with a 30-day delayed period in: (*a*) October, (*b*) November, and (*c*) December. The average number of floating particles per 1/4° × 1/4° grid cell is displayed as a color map, with corresponding scales shown on the right-hand side of each panel. Beached particles are represented by white circles, plotted per 1/10° × 1/10° grid cell, with scale references provided in the upper right box. Wind vectors and wind speed values for each month are also overlaid.

northeastward-flowing Kuroshio Current further facilitates the offshore transport of re-drifting litter.

In contrast, the semi-enclosed nature of the GoT and the absence of persistent, intense alongshore currents like the Kuroshio Current mean that re-drifting beach litter is less likely to be rapidly carried away. Instead of mid-latitude cyclonic activity, the GoT is subject to alternating NE and SW monsoons, which are dominant atmospheric systems in the subtropics and tropics. These seasonal monsoon winds are key drivers of debris transport, acting on an annual cycle, as well as phytoplankton biomass across the GoT (Leenawarat et al., 2022). In shallow seas such as the GoT, wind interactions can create more dynamic conditions than in deeper oceanic regions (Simpson and Sharples, 2012), making monsoon-driven transport even more significant.

Supporting this perspective, Semcesen et al. (2025) studied wind-driven transport of microplastic debris in a large urban harbor (Toronto Harbour, Canada) using GPS-tracked bottle drifters during the summer of 2021. They designed the drifter's shape and weight to resemble floating debris. Results showed that wind significantly influenced drifter movement, with trajectories and accumulation zones matching observed anthropogenic debris. Drifters moved two to five times faster than expected in small waterbodies and up to seven times faster in Lake Ontario, demonstrating strong wind dependence in both speed and direction. In fact, the second experiment with re-drifting due to offshore-ward winds could reproduce the prominent winter peak found by the visual observations in the GoT when we employed 30–60 days for delayed periods (Fig. 5). The present PTM experiment suggested that the delayed period of 10 days was also acceptable if the number of floating plastic debris in July is larger than that during winter in the

actual GoT.

Although a delayed period of 10–60 days is likely to occur under actual coastal conditions, such as mangroves with entangled roots, mudflats, vegetation, and sandy beaches, it remains challenging to determine the specific delayed period applicable to GoT. Previous studies support these results. Ivar do Sul et al. (2014) studied the retention and exportation of plastic debris by mangrove forest patches in northeastern Brazil by releasing color-tagged plastic items in various mangrove habitats. They found that plastic debris can be retained in mangroves for at least six months and potentially much longer. To better estimate the delayed period of beached plastic re-entering the ocean in the GoT, further studies should consider conducting mark-recapture experiments similar to those carried out by Kataoka et al. (2013). In such experiments, a selected beach along the eastern GoT coast could be cleared of all debris to initialize conditions. Newly stranded debris would then be individually marked each month with the date of stranding, enabling long-term tracking of persistence and replacement patterns. Monthly surveys of marked items would provide time series data that could be analyzed using the remnant function approach (Kataoka et al., 2013) to estimate e-folding times, interpreted as average residual times for beached debris. In turn, these values—especially when considered alongside wind regime changes—could serve as a basis for defining realistic delayed periods in future PTM experiments.

Moreover, to strengthen the model-data comparison, additional onboard visual surveys are recommended during key periods with limited observational coverage—particularly during the mid-SW monsoon season (June and July; Fig. 4). These surveys would help characterize seasonal variability in floating plastic debris abundance, offering crucial input for validating model outputs and narrowing the plausible range of delayed periods used in particle tracking models.

5. Conclusion

This study demonstrated that the particle tracking model (PTM), incorporating ocean–beach particle exchange driven by offshore winds, successfully reproduced the observed winter peak of floating plastic debris in the GoT. A delayed period of 1–2 months was appropriate for modeling the re-drifting process, although a shorter delay of around 10 days may also be valid if summer debris levels exceed those in winter. While riverine inputs remain a primary source of floating marine debris in the GoT, our findings underscore the significant role of beaches as secondary sources, particularly during the NE monsoon. In particular, the eastern beaches emerge as key contributors to debris re-drifting, driven by seasonal wind patterns.

Debris stranded on beaches may also be removed through beach cleaning activities, especially in popular tourist destinations. Such interventions can permanently remove debris from the system, preventing its return to the ocean. Moreover, not all stranded debris re-drift; some may remain on beaches for extended periods due to entrapment in vegetation, burial in sand, or other stabilizing factors. These processes, largely unaccounted for in the current model, could contribute to discrepancies between simulated and observed debris distributions, particularly in areas with active human intervention or strong retention conditions. Future modeling efforts should incorporate these potential sinks, including beach cleaning and long-term retention, to enhance simulation accuracy and better estimate the persistence and fate of plastic debris in coastal systems.

These findings emphasize the value of targeted, seasonally timed beach cleanup efforts—especially along the northern and eastern coasts—as a practical management strategy to reduce the re-entry of beached plastic debris. Incorporating both natural and human-driven processes into future PTM frameworks could further improve predictions and guide more effective marine debris mitigation policies. Such efforts could help lower the overall burden of floating plastics, improve coastal water quality, and support healthier marine ecosystems in the GoT.

CRediT authorship contribution statement

Hisayuki Arakawa: Data curation. **Sukchai Arnupapboon:** Data curation. **Nathacha Changphetphol:** Data curation. **Suchana Chavanich:** Investigation. **Voranop Viyakarn:** Investigation. **Pontipa Luadnakrob:** Writing – original draft, Visualization, Validation, Project administration, Methodology, Investigation, Formal analysis, Data curation. **María Belén Alfonso:** Writing – review & editing, Conceptualization. **Atsuhiko Isobe:** Writing – review & editing, Writing – original draft, Supervision, Funding acquisition, Conceptualization. **Tahira Irfan:** Software, Resources. **Keiichi Uchida:** Data curation.

Declaration of Competing Interest

The authors declare that they have no known competing financial interests or personal relationships that could have appeared to influence the work reported in this paper.

Acknowledgments

The authors would like to express their sincere gratitude to everyone who contributed to the field surveys conducted in this study. This research was supported by the Science and Technology Research Partnership for Sustainable Development (SATREPS), Japan, in collaboration with the Japan Science and Technology Agency (JST, JPMJSA1901) and Japan International Cooperation Agency (JICA), Thailand Science Research and Innovation Fund Chulalongkorn University (4710406), and Southeast Asian Fisheries Development Center, Training Department (SEAFDEC/TD).

Appendix A. Supporting information

Supplementary data associated with this article can be found in the online version at doi:10.1016/j.rsma.2025.104718.

Data availability

Data will be made available on request.

References

Amante, C., Eakins, B.W. 2009. ETOPO1 1 Arc-minute Global Relief Model: Procedures, Data Sources and Analysis, NOAA Technical Memorandum NESDIS NGDC-24, National Geophysical Data Center, NOAA. https://doi.org/10.7289/V5C8276M.

Anutaliya, A., 2023. Surface circulation in the Gulf of Thailand from remotely sensed observations: seasonal and interannual timescales. Ocean Sci. 19, 335–350. https://doi.org/10.5194/os-19-335-2023.

Asensio-Montesinos, F., Anfuso, G., Randerson, P., Williams, A.T., 2019. Seasonal comparison of beach litter on Mediterranean coastal sites (Alicante, SE Spain). Ocean Coast. Manag 181, 104914. https://doi.org/10.1016/j.ocecoaman.2019.104914.

Donelan, M.A., Curcic, M., Chen, S.S., Magnusson, A.F., 2012. Modeling waves and wind stress. J. Geophys. Res. 117. https://doi.org/10.1029/2011JC007787.

ESCAP. 2022. Closing the loop on plastic pollution in Nakorn Si Thammarat, Thailand. ⟨https://unescap.org/sites/default/d8files/event-documents/NST%20Baseline%20Report_0.pdf?utm_source=chatgpt.com⟩. (accessed 17 December 2024).

Guo, J., Qu, D., Zhang, Z., Sangmanee, C., Chanthasiri, N., Guo, B., 2021. Thermohaline conditions and circulation in the Gulf of Thailand during the northeast monsoon. Cont. Shelf Res. 225, 104487. https://doi.org/10.1016/J.csr.2021.104487.

Harris, P.T., Westerveld, L., Nyberg, B., Maes, T., Macmillan-Lawler, M., Appelquist, L.R., 2021. Exposure of coastal environments to river-sourced plastic pollution. Sci. Total Environ. 769, 145222. https://doi.org/10.1016/j.scitotenv.2021.145222.

Hinata, H., Mori, K., Ohno, K., Miyao, Y., Kataoka, T., 2017. An estimation of the average residence times and onshore-offshore diffusivities of beached microplastics based on the population decay of tagged meso- and macrolitter. Mar. Pollut. Bull. 122, 17–26. https://doi.org/10.1016/j.marpolbul.2017.05.012.

Irfan, T., Isobe, A., Matsuura, H., 2024. A particle tracking model approach to determine the dispersal of riverine plastic debris released into the Indian Ocean. Mar. Pollut. Bull. 199, 115985. https://doi.org/10.1016/j.marpolbul.2023.115985.

Isobe, A., Iwasaki, S., 2022. The fate of missing ocean plastics: are they just a marine environmental problem? Sci. Total Environ. 825, 153935. https://doi.org/10.1016/j.scitotenv.2022.153935.

Isobe, A., Kako, S., Chang, P., Matsuno, T., 2009. Two-way particle-tracking model for specifying sources of drifting objects: application to the East China Sea Shelf. J. Atmos. Ocean. Technol. 26, 1672–1682. https://doi.org/10.1175/2009JTECHO643.1.

Ivar do Sul, J.A., Costa, M.F., Silva-Cavalcanti, S., Araújo, M.C.B., 2014. Plastic debris retention and exportation by a mangrove forest patch. Mar. Pollut. Bull. 78, 252–257. https://doi.org/10.1016/j.marpolbul.2013.11.011.

Jambeck, J.R., Geyer, R., Wilcox, C., Siegler, T.R., Perryman, M., Andrady, A., Narayan, R., Law, K.L., 2015. Plastic waste inputs from land into the ocean. Science 347, 768–771. https://doi.org/10.1126/science.1260352.

Kako, S., Isobe, A., Kataoka, T., Yufu, K., Sugizono, S., Plybon, C., Murphy, T.A., 2018. Sequential webcam monitoring and modeling of marine debris abundance. Mar. Pollut. Bull. 132, 33–43. https://doi.org/10.1016/j.marpolbul.2018.04.075.

Kako, S., Isobe, A., Yoshioka, S., Chang, P.H., Matsuno, T., Kim, S.H., Lee, J.S., 2010. Technical issues in modeling surface-drifter behavior on the East China Sea shelf. J. Oceano 66. https://doi.org/10.1007/s10872-010-0014-z.

Kataoka, T., Hinata, H., Kato, S., 2013. Analysis of a beach as a time-invariant linear input/output system of marine litter. Mar. Pollut. Bull. 77, 266–273. https://doi.org/10.1016/j.marpolbul.2013.09.049.

Kuroda, M., Isobe, A., Uchida, K., Tokai, T., Kitakado, T., Yoshitake, M., Miyamoto, Y., Mukai, T., Imai, K., Shimizu, K., Yagi, M., Mituhasi, T., Habano, A., 2024. Abundance and potential sources of floating polystyrene foam macro- and microplastics around Japan. Sci. Total Environ. 925. https://doi.org/10.1016/j.scitotenv.2024.171421.

Lebreton, L.C.M., van der Zwet, J., Damsteeg, J.W., Slat, B., Andrady, A., Reisser, J., 2017. River plastic emissions to the world's oceans. Nat. Commun. 8, 15611. https://doi.org/10.1038/ncomms15611.

Leenawarat, D., Luang-on, J., Buranapratheprat, A., Ishizaka, J., 2022. Influences of tropical monsoon and El Niño Southern Oscillations on surface chlorophyll-a variability in the Gulf of Thailand. Front. Clim. 4, 936011. https://doi.org/10.3389/fclim.2022.936011.

Monchanin, C., Desmolles, M., Rivertta, K., Saramul, S., Charoenpong, C., Metrotra, R., 2024. Spatiotemporal variations in marine macro-litter pollution along the shoreline of Koh Mun Nai, an uninhabited island in the Gulf of Thailand. Environ. Pollut. 352. https://doi.org/10.1016/j.envpol.2024.124098.

Nakano, H., Alfonso, M.B., Jandang, S., Phinchan, N., Chavanich, S., Viyakarn, V., Isobe, A., 2024. Influence of monsoon seasonality and tidal cycle on microplastic presence and distribution in the Upper Gulf of Thailand. Sci. Total Environ. 920. https://doi.org/10.1016/j.scitotenv.2024.170787.

Narenpitak, P., Tomkratoke, S., Sirisup, S., Kongkulsiri, S., 2025. Projected sea level rise in Thailand: regional effects of climate change and solar radiation modification based on observations and the GeoMIP6. Elem. Sci. Anth 13 (1). https://doi.org/10.1525/elementa.2024.00069.

Okubo, A., 1971. Oceanic diffusion diagrams. Deep Sea Res. Oceanogr. Abstr. 18, 789–802. https://doi.org/10.1016/0011-7471(71)90046-5.

Randriarilala, F., Kitakado, T., Shiode, D., Sakaguchi, M., Hayashi, T., Tokai, T., 2014. Density estimation of the giant jellyfish *Nemopilema nomurai* around Japan using an alternative modified detection function for left truncation in a line transect survey. Fish. Sci. 80 (2), 261–271. https://doi.org/10.1007/s12562-013-0696-4.

Richardson, P.I., 1997. Drifting in the wind: leeway error in shipdrift data. DeepSea Res. I Oceanogr. Res. 44. https://doi.org/10.1016/S0967-0637(97)00059-9.

Saramul, S., Ezer, T., 2014. Spatial variations of sea level along the coast of Thailand: Impacts of extreme land subsidence, earthquakes and the seasonal monsoon. Glob. Planet. Change 122, 70–81. https://doi.org/10.1016/j.gloplacha.2014.08.012.

Semcesen, P.O., sherlock, C., Gutierrez, R.F., Rochman, C., Wells, M.G., 2025. Wind driven transport of microplastic debris in a large urban habour measured by GPS-tracked drifters. Mar. Pollut. Bull. https://doi.org/10.2139/ssrn.5072575.

Simpson, J., Sharples, J., 2012. Introduction to the Physical and Biological Oceanography of Shelf Seas. Cambridge University Press, Cambridge.

Tomita, H., Hihara, T., Kako, S., Kubota, M., Kutsuwada, K., 2019. An introduction to J-OFURO3, a third-generation Japanese ocean flux data set using remote-sensing observations. J. Oceano 75, 171–194. https://doi.org/10.1007/s10872-018-0493-x.

Trajano, J.C., 2023. Turn. tide Southeast Asia'S. Plast. Pollut. Crisis Policy Rep. ⟨https://www.rsis.edu.sg/wp-content/uploads/2023/02/PR230228_Turning-the-Tide-on-Southeast-Asias-Plastic-Pollution-Crisis.pdf⟩.

UN Environment program and COBSEA, SEA circular country profile for Thailand. 2023. ⟨http://sea-circular.org/country/thailand/⟩ (accessed 23 January 2025).

Van Emmerik, T., Steady, E., Kieu-Le, T.C., Nguyen, L., Gratiot, N., 2019. Seasonality of riverine macroplastic transport. Nat. Res. https://doi.org/10.1038/s41598-019-50096-1.

Williams, A.T., Tudor, D.T., 2001. Litter burial and exhumation: spatial and temporal distribution on a cobble pocket beach. Mar. Pollut. Bull. 42, 1031–1039. https://doi.org/10.1016/S0025-326X(01)00058-3.

Williams, A.T., Simmons, S.L., 1996. The degradation of plastic litter in the rivers: implications for beaches. J. Coast. Conserv. 2, 63–72. https://doi.org/10.1007/BF02743038.

Yin, C.S., Chai, Y.J., Danielle, C., Yusri, Y., Barry, G.J., 2020. Anthropogenic marine debris accumulation in mangroves on Penang Island, Malaysia. J. Sustain. Sci. Manag. 15. https://doi.org/10.46754/jssm.2020.08.004.

Zhang, P., Wei, S., Zhang, J., Zhong, H., Wang, S., Jian, Q., 2022. Seasonal distribution, composition, and inventory of plastic debris on the Yugang park beach in Zhanjiang Bay. Int. J. Environ. Res. Public Health 19, 4886. https://doi.org/10.3390/ijerph19084886.